

PALM: An Incremental Construction of Hyperplanes for Data Stream Regression

Md Meftahul Ferdaus, *Student Member, IEEE*, Mahardhika Pratama, *Member, IEEE*, Sreenatha G. Anavatti, Matthew A. Garratt,

arXiv:1805.04258v2 [cs.NE] 28 Aug 2018

Abstract—Data stream has been the underlying challenge in the age of big data because it calls for real-time data processing with the absence of a retraining process and/or an iterative learning approach. In realm of fuzzy system community, data stream is handled by algorithmic development of self-adaptive neuro-fuzzy systems (SANFS) characterized by the single-pass learning mode and the open structure property which enables effective handling of fast and rapidly changing natures of data streams. The underlying bottleneck of SANFSs lies in its design principle which involves a high number of free parameters (rule premise and rule consequent) to be adapted in the training process. This figure can even double in the case of type-2 fuzzy system. In this work, a novel SANFS, namely parsimonious learning machine (PALM), is proposed. PALM features utilization of a new type of fuzzy rule based on the concept of hyperplane clustering which significantly reduces the number of network parameters because it has no rule premise parameters. PALM is proposed in both type-1 and type-2 fuzzy systems where all of which characterize a fully dynamic rule-based system. That is, it is capable of automatically generating, merging and tuning the hyperplane-based fuzzy rule in the single pass manner. Moreover, an extension of PALM, namely recurrent PALM (rPALM), is proposed and adopts the concept of teacher-forcing mechanism in the deep learning literature. The efficacy of PALM has been evaluated through numerical study with six real-world and synthetic data streams from public database and our own real-world project of autonomous vehicles. The proposed model showcases significant improvements in terms of computational complexity and number of required parameters against several renowned SANFSs, while attaining comparable and often better predictive accuracy.

Index Terms—data stream, fuzzy, hyperplane, incremental, learning machine, parsimonious

I. INTRODUCTION

ADVANCE in both hardware and software technologies has triggered generation of a large quantity of data in an automated way. Such applications can be exemplified by space, autonomous systems, aircraft, meteorological analysis, stock market analysis, sensors networks, users of the internet, etc., where the generated data are not only massive and possibly unbounded but also produced at a rapid rate under complex environments. Such online data are known as data stream [1], [2]. A data stream can be expressed in a more

formal way [3] as $S = \{x^1, x^2, \dots, x^i, \dots, x^\infty\}$, where x^i is enormous sequence of data objects and possibly unbounded. Each of the data object can be defined by an n dimensional feature vector as $x^i = [x_j^i]_{j=1}^n$, which may belong to a continuous, categorical, or mixed feature space. In the field of data stream mining, developing a learning algorithm as a universal approximator is challenging due to the following factors 1) the whole data to train the learning algorithm is not readily available since the data arrive continuously; 2) the size of a data stream is not bounded; 3) dealing with a huge amount of data; 4) distribution of the incoming unseen data may slide over time slowly, rapidly, abruptly, gradually, locally, globally, cyclically or otherwise. Such variations in the data distribution of data streams over time are known as *concept drift* [4], [5]; 5) data are discarded after being processed to suppress memory consumption into practical level.

To cope with above stated challenges in data streams, the learning machine should be equipped with the following features: 1) capability of working in single pass mode; 2) handling various concept drifts in data streams; 3) has low memory burden and computational complexity to enable real-time deployment under resource constrained environment. In realm of fuzzy system, such learning aptitude is demonstrated by Self Adaptive Neuro-Fuzzy System (SANFS) [6]. Until now, existing SANFSs are usually constructed via hypersphere-based or hyperellipsoid-based clustering techniques (HSBC or HESC) to automatically partition the input space into a number of fuzzy rule and rely on the assumption of normal distribution due to the use of Gaussian membership function [7]–[15]. As a result, they are always associated with rule premise parameters, the mean and width of Gaussian function, which need to be continuously adjusted. This issue complicates its implementation in a complex and deep structure. As a matter of fact, existing neuro-fuzzy systems can be seen as a single hidden layer feedforward network. Other than the HSSC or HESC, the data cloud based clustering (DCBC) concept is utilized in [16], [17] to construct the SANFS. Unlike the HSSC and HESC, the data clouds do not have any specific shape. Therefore, required parameters in DCBC are less than HSSC and HESC. However, in DCBC, parameters like mean, accumulated distance of a specific point to all other points need to be calculated. In other words, it does not offer significant reduction on the computational complexity and memory demand of SANFS. Hyperplane-Based Clustering (HPBC) provides a promising avenue to overcome this drawback because it bridges the rule premise and the rule consequent by means of the hyperplane construction.

Md Meftahul Ferdaus, Sreenatha G. Anavatti, and Matthew A. Garratt are with the School of Engineering and Information Technology, University of New South Wales at the Australian Defence Force Academy, Canberra, ACT 2612, Australia (e-mail: m.ferdaus@student.unsw.edu.au; s.anavatti@adfa.edu.au; M.Garratt@adfa.edu.au).

Mahardhika Pratama is with the School of Computer Science and Engineering, Nanyang Technological University, Singapore, 639798, Singapore (e-mail: mpratama@ntu.edu.sg).

Although the concept of HPBC already exists since the last two decades [18]–[20], all of them are characterized by a static structure and are not compatible for data stream analytic due to their offline characteristics. Besides, majority of these algorithms still use the Gaussian or bell-shaped Gaussian function [21] to create the rule premise and are not free of the rule premise parameters. This problem is solved in [22], where they have proposed a new function to accommodate the hyperplanes directly in the rule premise. Nevertheless, their model also exhibit a fixed structure and operates in the batch learning node. Based on this research gap, a novel SANFS, namely parsimonious learning machine (PALM), is proposed in this work. The novelty of this work can be summarized as follows:

- 1) PALM is constructed using the HPBC technique and its fuzzy rule is fully characterized by a hyperplane which underpins both the rule consequent and the rule premise. This strategy reduces the rule base parameter to the level of $C * (P + 1)$ where C, P are respectively the number of fuzzy rule and input dimension.
- 2) PALM is proposed in both type-1 and type-2 versions derived from the concept of type-1 and type-2 fuzzy systems. Type-1 version incurs less network parameters and faster training speed than the type-2 version whereas type-2 version expands the degree of freedom of the type-1 version by applying the interval-valued concept leading to be more robust against uncertainty than the type-1 version.
- 3) PALM features a fully open network structure where its rules can be automatically generated, merged and updated on demand in the one-pass learning fashion. The rule generation process is based on the self-constructing clustering approach [23], [24] checking coherence of input and output space. The rule merging scenario is driven by the similarity analysis via the distance and orientation of two hyperplanes. The online hyperplane tuning scenario is executed using the fuzzily weighted generalized recursive least square (FWGRLS) method.
- 4) an extension of PALM, namely recurrent PALM (rPALM), is put forward in this work. rPALM addresses the underlying bottleneck of HPBC method: dependency on target variable due to the definition of point-to-hyperplane distance [25]. This concept is inspired by the teacher forcing mechanism in the deep learning literature where activation degree of a node is calculated with respect to predictor's previous output. The performance of rPALM has been numerically validated in our supplemental document where its performance is slightly inferior to PALM but still highly competitive to most prominent SANFSs in terms of accuracy.
- 5) Two real-world problems from our own project, namely online identification of Quadcopter unmanned aerial vehicle (UAV) and helicopter UAV, are presented in this paper and exemplify real-world streaming data problems. The two datasets are collected from indoor flight tests in the UAV lab of the university of new south wales (UNSW), Canberra campus. These datasets, PALM and

rPALM codes are made publicly available in [26].

The efficacy of both type-1 and type-2 PALMs have been numerically evaluated using six real-world and synthetic streaming data problems. Moreover, PALM is also compared against prominent SANFSs in the literature and demonstrates encouraging numerical results in which it generates compact and parsimonious network structure while delivering comparable and even better accuracy than other benchmarked algorithms.

The remainder of this paper is structured as follows: Section II discusses literature survey over closely related works. In Section III, The network architecture of both type-1 and type-2 PALM are elaborated. Section IV describes the online learning policy of type-1 PALM, while Section V presents online learning mechanism of type-2 PALM. In Section VI, the proposed PALM's efficacy has been evaluated through real-world and synthetic data streams. Finally, the paper ends by drawing the concluding remarks in Section VII.

II. RELATED WORK AND RESEARCH GAP WITH THE STATE-OF-THE-ART ALGORITHMS

SANFS can be employed for data stream regression, since they can learn from scratch with no base knowledge and are embedded with the self-organizing property to adapt to the changing system dynamics [27]. It fully work in a single-pass learning scenario, which is efficient for online learning under limited computational resources. An early work in this domain is seen in [6] where an SANFS, namely SONFIN, was proposed. Evolving clustering method (ECM) is implemented in [28] to evolve fuzzy rules. Another pioneering work in this area is the development of the online evolving T-S fuzzy system namely eTS [7] by Angelov. eTS has been improved in the several follow-up works: eTS+ [29], Simpl_eTS [8], AnYa [16]. However, eTS+, and Simpl_eTS generate axis parallel ellipsoidal clusters, which cannot deal effectively with non-axis parallel data distribution. To deal with the non-axis parallel data distribution, an evolving multi-variable Gaussian (eMG) function was introduced in the fuzzy system in [30]. Another example of SANFS exploiting the multivariable Gaussian function is found in [10] where the concept of statistical contribution is implemented to grow and prune the fuzzy rules on the fly. This work has been extended in [9] where the idea of statistical contribution is used as a basis of input contribution estimation for the online feature selection scenario.

The idea of SANFS was implemented in type-2 fuzzy system in [31]. Afterward, they have extended their concept in local recurrent architecture [32], and interactive recurrent architecture [33]. These works utilize Karnik-Mendel (KM) type reduction technique [34], which relies on an iterative approach to find left-most and right-most points. To mitigate this shortcoming, the KM type reduction technique can be replaced with q design coefficient [35] introduced in [36]. SANFS is also introduced under the context of metacognitive learning machine (McLM) which encompasses three fundamental pillars of human learning: what-to-learn, how-to-learn, when-to-learn. The idea of McLM was introduced in [37]. McLM has been modified with the use of Scaffolding theory, McSLM, which aims to realize the plug-and-play learning

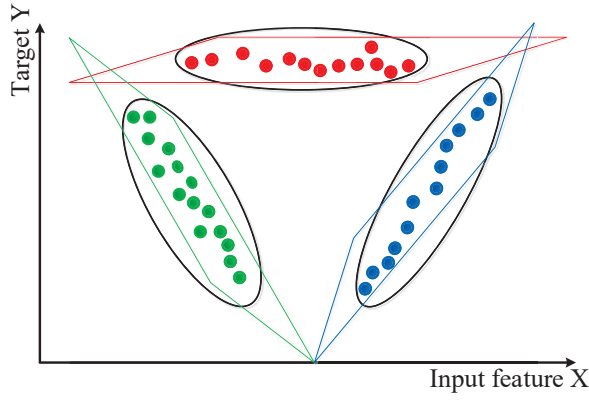


Figure 1. Clustering in T-S fuzzy model using hyperplanes

fashion [38]. To solve the problem of uncertainty, temporal system dynamics and the unknown system order McSLM was extended in recurrent interval-valued metacognitive scaffolding fuzzy neural network (RIVMcSFNN) [11]. The vast majority of SANFSs are developed using the concept of HSSC and HESC which impose considerable memory demand and computational burden because both rule premise and rule consequent have to be stored and evolved during the training process.

III. NETWORK ARCHITECTURE OF PALM

In this section, the network architecture of PALM is presented in details. The T-S fuzzy system is a commonly used technique to approximate complex nonlinear systems due to its universal approximation property. The rule base in the T-S fuzzy model of that multi-input single-output (MISO) system can be expressed in the following IF-THEN rule format:

$$R^j : \text{ If } x_1 \text{ is } B_1^j \text{ and } x_2 \text{ is } B_2^j \text{ and...and } x_n \text{ is } B_n^j \\ \text{ Then } y_j = b_{0j} + a_{1j}x_1 + \dots + a_{nj}x_n \quad (1)$$

where R^j stands for the j th rule, $j = 1, 2, 3, \dots, R$, and R indicates the number of rules, $i = 1, 2, \dots, n$; n denotes the dimension of input feature, x_n is the n th input feature, a and b are consequent parameters of the sub-model belonging to the j th rule, y_j is the output of the j th sub-model. The T-S fuzzy model can approximate a nonlinear system with a combination of several piecewise linear systems by partitioning the entire input space into several fuzzy regions. It expresses each input-output space with a linear equation as presented in (1). Approximation using T-S fuzzy model leads to a nonlinear programming problem and hinders its practical use. A simple solution to the problem is the utilization of various clustering techniques to identify the rule premise parameters. Because of the generation of the linear equation in the consequent part, the HPBC can be applied to construct the T-S fuzzy system efficiently. The advantages of using HPBC in the T-S fuzzy model can be seen graphically in Fig. 1.

Some popular algorithms with HPBC are fuzzy C-regression model (FCRM) [39], fuzzy C-quadratic shell (FCQS) [40],

double FCM [18], inter type-2 fuzzy c-regression model (IT2-FCRM) [22]. A main limitation of these algorithms is their non-incremental nature which does not suit for data stream regression. Moreover, they still deploy Gaussian function to represent the rule premise of TS fuzzy model which does not exploit the parameter efficiency trait of HPBC. To fill up this research gap, a new membership function [22] is proposed to accommodate the use of hyperplanes in the rule premise part of TS fuzzy system. It can be expressed as:

$$\mu_B(j) = \exp\left(-\Gamma \frac{dst(j)}{\max(dst(j))}\right) \quad (2)$$

where $j = 1, 2, \dots, R$; R is the number of rules, Γ is an adjustment parameter which controls the fuzziness of membership grades. Based on the observation in [22], and empirical analysis with variety of data streams in our work, the range of Γ is settled as $[1, 100]$. $dst(j)$ denotes the distance from present sample to the j th hyperplane. In our work, $dst(j)$ is defined as [22] as follows:

$$dst(j) = \frac{|X_t \omega_j|}{\|\omega_j\|} \quad (3)$$

where $X_t \in \mathbb{R}^{1 \times (n+1)}$ and $\omega_j \in \mathbb{R}^{(n+1) \times 1}$ respectively stand for the input vector of the t th observation and the output weight vector of the j th rule. This membership function enables the incorporation of HPBC directly into the T-S fuzzy system directly with the absence of rule parameters except the first order linear function or hyperplane. Because a point to plane distance is not unique, the compatibility measure is executed using the minimum point to plane distance. The following discusses the network structure of PALM encompassing its type-1 and type-2 versions. PALM can be modeled as a four-layered network working in tandem, where the fuzzy rule triggers a hyperplane-shaped cluster and is induced by (3). Since T-S fuzzy rules can be developed solely using a hyperplane, PALM is free from antecedent parameters which results in dramatic reduction of network parameters. Furthermore, it operates in the one-pass learning fashion where it works point by point and a data point is discarded directly once learned.

A. Structure of Type-1 PALM Network:

In type-1 PALM network architecture, the membership function exposed in (2) is utilized to fit the hyperplane-shaped cluster in identifying type-1 T-S fuzzy model. To understand the work flow let us consider that a single data point x_n is fed into PALM at the n -th observation. Appertaining to the concept of type-1 fuzzy system, this crisp data needs to be transformed to fuzzy set. This fuzzification process is attained using type-1 hyperplane-shaped membership function, which is framed through the concept of point-to-plane distance. This hyperplane-shaped type-1 membership function can be expressed as:

$$f_{T1}^1 = \mu_B(j) = \exp\left(-\Gamma \frac{dst(j)}{\max(dst(j))}\right) \quad (4)$$

where $dst(j)$ in (4) denotes the distance between the current sample and j th hyperplane as with (3). It is defined as per definition of a point-to-plane distance [25] and is formally expressed as follows:

$$dst(j) = \left| \frac{y_d - (\sum_{i=1}^n a_{ij}x_i + b_{0j})}{\sqrt{1 + \sum_{i=1}^n (a_{ij})^2}} \right| \quad (5)$$

where a_{ij} and b_{0j} are consequent parameters of the j th rule, $i = 1, 2, \dots, n$; n is the number of input dimension, and y_d is the target variable. The exertion of y_d is an obstruction for PALM due to target variable's unavailability in testing phase. This issue comes into picture due to the definition of a point-to-hyperplane distance [25]. To eradicate such impediment, a recurrent PALM (RPALM) framework is developed here. We refer curious readers to the supplementary document for details on the RPALM. Considering a MISO system, the IF-THEN rule of type-1 PALM can be expressed as follows:

$$R^j : \text{ IF } X_n \text{ is close to } f_{T1_j}^2 \text{ THEN } y_j = x_e^j \omega_j \quad (6)$$

where x_e is the extended input vector and is expressed by inserting the intercept to the original input vector as $x_e = [1, x_1^k, x_2^k, \dots, x_n^k]$, ω_j is the weight vector for the j th rule, y_j is the consequent part of the j th rule. Since type-1 PALM has no premise parameters, the antecedent part is simply hyperplane. It is observed from (6) that the drawback of HPBC-based TS fuzzy system lies in the high level fuzzy inference scheme which degrades the transparency of fuzzy rule. The intercept of extended input vector controls the slope of hyperplane which functions to prevent the untypical gradient problem.

The consequent part is akin to the basic T-S fuzzy model's rule consequent part ($y_j = b_{0j} + a_{1j}x_1 + \dots + a_{nj}x_n$). The consequent part for the j th hyperplane is calculated by weighting the extended input variable (x_e) with its corresponding weight vector as follows:

$$f_{T1_j}^2 = x_e^T \omega_j \quad (7)$$

It is used in (7) after updating recursively by the FWGRSL method, which ensures a smooth change in the weight value. In the next step, the rule firing strength is normalized and combined with the rule consequent to produce the end-output of type-1 PALM. The final crisp output of the PALM for type-1 model can be expressed as follows:

$$f_{T1}^3 = \frac{\sum_{j=1}^R f_{T1_j}^1 f_{T1_j}^2}{\sum_{i=1}^R f_{T1_i}^1} \quad (8)$$

The normalization term in (8) guarantees the partition of unity where the sum of normalized membership degree is unity. The T-S fuzzy system is functionally-equivalent to the radial basis function (RBF) network if the rule firing strength is directly connected to the output of the consequent layer [41]. It is also depicted that the final crisp output is produced by the weighted average defuzzification scheme.

B. Network structure of the Type-2 PALM :

Type-2 PALM differs from the type-1 variant in the use of interval-valued hyperplane generating the type-2 fuzzy rule. Akin to its type-1 version, type-2 PALM starts operating by intaking the crisp input data stream x_n to be fuzzied. Here, the fuzzification occurs with help of interval-valued hyperplane based membership function, which can be expressed as:

$$\tilde{f}_{out}^1 = \exp \left(-\Gamma \frac{\tilde{dst}(j)}{\max(\tilde{dst}(j))} \right) \quad (9)$$

where $\tilde{f}_{out}^1 = [\underline{f}_{out}^1, \overline{f}_{out}^1]$ is the upper and lower hyperplane, $\tilde{dst}(j) = [\underline{dst}(j), \overline{dst}(j)]$ is interval valued distance, where $\overline{dst}(j)$ is the distance between present input samples and j th upper hyperplane, and $\underline{dst}(j)$ is that between present input samples and j th lower hyperplane. In type-2 architecture, distances among incoming input data and upper and lower hyperplanes are calculated as follows:

$$\tilde{dst}(j) = \left| \frac{y_d - (\sum_{i=1}^n \tilde{a}_{ij}x_i + \tilde{b}_{0j})}{\sqrt{1 + \sum_{i=1}^n (\tilde{a}_{ij})^2}} \right| \quad (10)$$

where $\tilde{a}_{ij} = [\underline{a}_{ij}; \overline{a}_{ij}]$ and $\tilde{b}_{0j} = [\underline{b}_{0j}; \overline{b}_{0j}]$ are the interval-valued coefficients of the rule consequent of type-2 PALM. Like the type-1 variants, type-2 PALM has dependency on target value (y_d). Therefore, they are also extended into type-2 recurrent structure and elaborated in the supplementary document. The use of interval-valued coefficients result in the interval-valued firing strength which forms the footprint of uncertainty (FoU). The FoU is the key component against uncertainty of data streams and sets the degree of tolerance against uncertainty.

In a MISO system, the IF-THEN rule of type-2 PALM can be expressed as:

$$R^j : \text{ IF } X_n \text{ is close to } \tilde{f}_{out}^2 \text{ THEN } y_j = x_e^j \tilde{\omega}_j \quad (11)$$

where x_e is the extended input vector, $\tilde{\omega}_j$ is the interval-valued weight vector for the j th rule, y_j is the consequent part of the j th rule, whereas the antecedent part is merely interval-valued hyperplane. The type-2 fuzzy rule is similar to that of the type-1 variant except the presence of interval-valued firing strength and interval-valued weight vector. In type-2 PALM, the consequent part is calculated by weighting the extended input variable x_e with the interval-valued output weight vectors $\tilde{\omega}_j = [\underline{\omega}_j, \overline{\omega}_j]$ as follows:

$$\overline{f}_{out_j}^2 = x_e^j \overline{\omega}_j, \quad \underline{f}_{out_j}^2 = x_e^j \underline{\omega}_j \quad (12)$$

The lower weight vector $\underline{\omega}_j$ for the j th lower hyperplane, and upper weight vector $\overline{\omega}_j$ for the j th upper hyperplane are initialized by allocating higher value for upper weight vector than the lower weight vector. These vectors are updated recursively by FWGRSL method, which ensures a smooth change in weight value.

Before performing the defuzzification method, the type reduction mechanism is carried out to craft the type-reduced

set - the transformation from the type-2 fuzzy variable to the type-1 fuzzy variable. One of the commonly used type-reduction method is the Karnik Mendel (KM) procedure [34]. However, in the KM method, there is an involvement of an iterative process due to the requirement of reordering the rule consequent first in ascending order before getting the cross-over points iteratively incurring expensive computational cost. Therefore, instead of the KM method, the q design factor [35] is utilized to orchestrate the type reduction process. The final crisp output of the type-2 PALM can be expressed as follows:

$$f_{out}^3 = y_{out} = \frac{1}{2} (y_{l_{out}} + y_{r_{out}}) \quad (13)$$

where

$$y_{l_{out}} = \frac{\sum_{j=1}^R q_l f_{out}^1 f_{out}^2}{\sum_{i=1}^R \bar{f}_{out}^1} + \frac{\sum_{j=1}^R (1 - q_l) \bar{f}_{out}^1 f_{out}^2}{\sum_{i=1}^R f_{out}^1} \quad (14)$$

$$y_{r_{out}} = \frac{\sum_{j=1}^R q_r f_{out}^1 \bar{f}_{out}^2}{\sum_{i=1}^R \bar{f}_{out}^1} + \frac{\sum_{j=1}^R (1 - q_r) \bar{f}_{out}^1 \bar{f}_{out}^2}{\sum_{i=1}^R f_{out}^1} \quad (15)$$

where $y_{l_{out}}$ and $y_{r_{out}}$ are the left and right outputs resulted from the type reduction mechanism. q_l and q_r , utilized in (14) and (15), are the design factors initialized in a way to satisfy the condition $q_l < q_r$. In our q design factor, the q_l and q_r steers the proportion of the upper and lower rules to the final crisp outputs $y_{l_{out}}$ and $y_{r_{out}}$ of the PALM. The normalization process of the type-2 fuzzy inference scheme [36] was modified in [11] to prevent the generation of the invalid interval. The generation of this invalid interval as a result of the normalization process of [36] was also proved in [11]. Therefore, normalization process as adopted in [11] is applied and advanced in terms of q_l and q_r in our work. Besides, in order to improve the performance of the proposed PALM, the q_l and q_r are not left constant rather continuously adapted using gradient decent technique as explained in section IV. Notwithstanding that the type-2 PALM is supposed to handle uncertainty better than its type-1 variant, it incurs a higher number of network parameters in the level of $2 \times R \times (n + 1)$ as a result of the use of upper and lower weight vectors $\bar{\omega}_j = [\underline{\omega}_j, \bar{\omega}_j]$. In addition, the implementation of q -design factor imposes extra computational cost because q_l and q_r call for a tuning procedure with the gradient descent method.

IV. ONLINE LEARNING POLICY IN TYPE-1 PALM

This section describes the online learning policy of our proposed type-1 PALM. PALM is capable of starting its learning process from scratch with an empty rule base. Its fuzzy rules can be automatically generated on the fly using the self constructive clustering (SCC) method which checks the input and output coherence. The complexity reduction mechanism is implemented using the hyperplane merging module which vets similarity of two hyperplanes using the distance and angle concept. The hyperplane-based fuzzy rule is adjusted using the FWGRLS method in the single-pass learning fashion.

A. Mechanism of Growing Rules

The rule growing mechanism of type-1 PALM is adopted from the self-constructive clustering (SSC) method developed in [23], [24] to adapt the number of rules. This method has been successfully applied to automatically generate interval-valued data clouds in [17] but its use for HPBC deserves an in-depth investigation. In this technique, the rule significance is measured by calculating the input and output coherence. The coherence is measured by analysing the correlation between the existing data samples and the target concept. Hereby assuming the input vector as $X_t \in \mathbb{R}^n$, target vector as $T_t \in \mathbb{R}^n$, hyperplane of the i th local sub-model as $\mathcal{H}_i \in \mathbb{R}^{1 \times (n+1)}$, the input and output coherence between $X_t \in \mathbb{R}^n$ and each $\mathcal{H}_i \in \mathbb{R}^{1 \times (n+1)}$ are calculated as follows:

$$I_c(\mathcal{H}_i, X_t) = \xi(\mathcal{H}_i, X_t) \quad (16)$$

$$O_c(\mathcal{H}_i, X_t) = \xi(X_t, T_t) - \xi(\mathcal{H}_i, T_t) \quad (17)$$

where $\xi(\cdot)$ express the correlation function. There are various linear and nonlinear correlation methods for measuring correlation, which can be applied. Among them, the nonlinear methods for measuring the correlation between variables are hard to employ in the online environment since they commonly use the discretization or Parzen window method. On the other hand, Pearson correlation is a widely used method for measuring correlation between two variables. However, it suffers from some limitations: it's insensitivity to the scaling and translation of variables and sensitivity to rotation [42]. To solve these problems, a method namely maximal information compression index (MCI) is proposed in [42], which has also been utilized in the SSC method to measure the correlation $\xi(\cdot)$ between variables as follows:

$$\xi(X_t, T_t) = \frac{1}{2} (\text{var}(X_t) + \text{var}(T_t)) - \sqrt{(\text{var}(X_t) + \text{var}(T_t))^2 - 4\text{var}(X_t)(T_t)(1 - \rho(X_t, T_t)^2)} \quad (18)$$

$$\rho(X_t, T_t) = \frac{\text{cov}(X_t, T_t)}{\sqrt{\text{var}(X_t)\text{var}(T_t)}} \quad (19)$$

where $\text{var}(X_t)$, $\text{var}(T_t)$ express the variance of X_t and T_t respectively, $\text{cov}(X_t, T_t)$ presents the covariance between two variables X_t and T_t , $\rho(X_t, T_t)$ stands for Pearson correlation index of X_t and T_t . In a similar way, the correlation $\xi(\mathcal{H}_i, X_t)$ and $\xi(\mathcal{H}_i, T_t)$ can be measured using (18) and (19). In addition, the MCI method measures the compressed information when a newly observed sample is ignored. Properties of the MCI method in our work can be expressed as follows:

- 1) $0 \leq \xi(X_t, T_t) \leq \frac{1}{2} (\text{var}(X_t) + \text{var}(T_t))$.
- 2) a maximum possible correlation is $\xi(X_t, T_t) = 0$.
- 3) express symmetric behavior $\xi(X_t, T_t) = \xi(T_t, X_t)$.
- 4) invariance against the translation of the dataset.
- 5) express the robustness against rotation.

$I_c(\mathcal{H}_i, X_t)$ is projected to explore the similarity between \mathcal{H}_i and X_t directly, while $O_c(\mathcal{H}_i, X_t)$ is meant to examine the dissimilarity between \mathcal{H}_i and X_t indirectly by utilizing the

target vector as a reference. In the present hypothesis, the input and output coherence need to satisfy the following conditions to add a new rule or hyperplane:

$$I_c(\mathcal{H}_i, X_t) > b_1 \quad \text{and} \quad O_c(\mathcal{H}_i, X_t) < b_2 \quad (20)$$

where $b_1 \in [0.01, 0.1]$, and $b_2 \in [0.01, 0.1]$ are predetermined thresholds. If the hypothesis satisfies both the conditions of (20), a new rule is added with the highest input coherence. Besides, the accommodated data points of a rule are updated as $N_{j^*} = N_{j^*} + 1$. Also, the correlation measure functions $\xi(\cdot)$ are updated with (18) and (19). Due to the utilization of the local learning scenario, each rule is adapted separately and therefore covariance matrix is independent to each rule $C_j(k) \in \mathbb{R}^{(n+1) \times (n+1)}$, here n is the number of inputs. When a new hyperplane is added by satisfying (20), the hyperplane parameters and the output covariance matrix of FWGRS method are crafted as follows:

$$\pi_{R+1} = \pi_{R^*}, \quad C_{R+1} = \Omega I \quad (21)$$

Due to the utilization of the local learning scenario, the consequent of the newly added rules can be assigned as the closest rule, since the expected trend in the local region can be portrayed easily from the nearest rule. The value of Ω in (21) is very large (10^5). The reason for initializing the C matrix with a large value is to obtain a fast convergence to the real solution [43]. The proof of such consequent parameter setting is detailed in [44]. In addition, the covariance matrix of the individual rule has no relationship with each other. Thus, when the rules are pruned in the rule merging module, the covariance matrix, and consequent parameters are deleted as it does not affect the convergence characteristics of the C matrix and consequent of remaining rules.

B. Mechanism of Merging Rules

In SANFS, the rule evolution mechanism usually generate redundant rules. These unnecessary rules create complicity in the rule base, which hinders some desirable features of fuzzy rules: transparency and tractability in their operation. Notably, in handling data streams, two overlapping clusters or rules may easily be obtained when new samples occupied the gap between the existing two clusters. Several useful methods have been employed to merge redundant rules or clusters in [9], [17], [29], [45]. However, all these techniques are appropriate for mainly hypersphere-based or ellipsoid-based clusters.

In realm of hyperplane clusters, there is a possibility of generating a higher number of hyperplanes in dealing with the same dataset than spherical or ellipsoidal clusters because of the nature of HPBC in which each hyperplane represents specific operating region of the approximation curve. This opens higher chance in generating redundant rules than HSSC and HESC. Therefore, an appropriate merging technique is vital and has to achieve tradeoff between diversity of fuzzy rules and generalization power of the rule base. To understand clearly, the merging of two hyperplanes due to the new incoming training data samples is illustrated in Fig. 2.

In [46], to merge the hyperplanes, the similarity and dissimilarity between them are obtained by measuring only the angle between the hyperplanes. This strategy is ,however, not conclusive to decide the similarity between two hyperplanes because it solely considers the orientation of hyperplane without looking at the relationship of two hyperplanes in the target space.

In our work, to measure the similarity between the hyperplane-shaped fuzzy rules, the angle between them is estimated as follows [9], [47]:

$$\theta_{hp} = \arccos \left(\left| \frac{\omega_R^T \omega_{R+1}}{|\omega_R| |\omega_{R+1}|} \right| \right) \quad (22)$$

where θ_{hp} is ranged between 0 and π radian, $\omega_R = [b_{1,R}, b_{2,R}, \dots, b_{k,R}]$, $\omega_{R+1} = [b_{1,R+1}, b_{2,R+1}, \dots, b_{k,R+1}]$. The angle between the hyperplanes is not sufficient to decide whether the rule merging scenario should take place because it does not inform the closeness of two hyperplanes in the target space. Therefore, the spatial proximity between two hyperplanes in the hyperspace are taken into account. If we consider two hyperplanes as $l_{R1} = a_1 + xb_1$, and $l_{R2} = a_2 + xb_2$, then the minimum distance between them can be projected as follows:

$$d_{R,R+1} = \left| (a_1 - a_2) \cdot \frac{(b_1 \times b_2)}{|b_1 \times b_2|} \right| \quad (23)$$

The rule merging condition is formulated as follows:

$$\theta_{hp} \leq c_1 \quad \text{and} \quad d_{R,R+1} \leq c_2 \quad (24)$$

where $c_1 \in [0.01, 0.1]$, $c_2 \in [0.001, 0.1]$ are predefined thresholds. If (24) is satisfied, fuzzy rules are merged. It is worth noting that the merging technique is only applicable in the local learning context because, in case of global learning, the orientation and similarity of two hyperplanes have no direct correlation to their relationship.

In our merging mechanism, a dominant rule having higher support is retained, whereas a less dominant hyperplane (rule) resided by less number of samples is pruned to mitigate the structural simplification scenario of PALM. A dominant rule has a higher influence on the merged cluster because it represents the underlying data distribution. That is, the dominant rule is kept in the rule base in order for good partition of data space to be maintained and even improved. For simplicity, the weighted average strategy is adopted in merging two hyperplanes as follows:

$$\omega_{acm}^{new} = \frac{\omega_{acm}^{old} N_{acm}^{old} + \omega_{acm+1}^{old} N_{acm+1}^{old}}{N_{acm}^{old} + N_{acm+1}^{old}} \quad (25)$$

$$N_{acm}^{new} = N_{acm}^{old} + N_{acm+1}^{old} \quad (26)$$

where ω_{acm}^{old} is the output weight vector of the acm th rule, ω_{acm+1}^{old} is the output weight vector of $(acm + 1)$ th rule, and ω_{acm}^{new} is the output weight vector of the merged rule, N is the population of a fuzzy rule. Note that the rule acm is more influential than the rule $acm + 1$, since $N_{acm} > N_{acm+1}$. The rule merging procedure is committed during the stable period

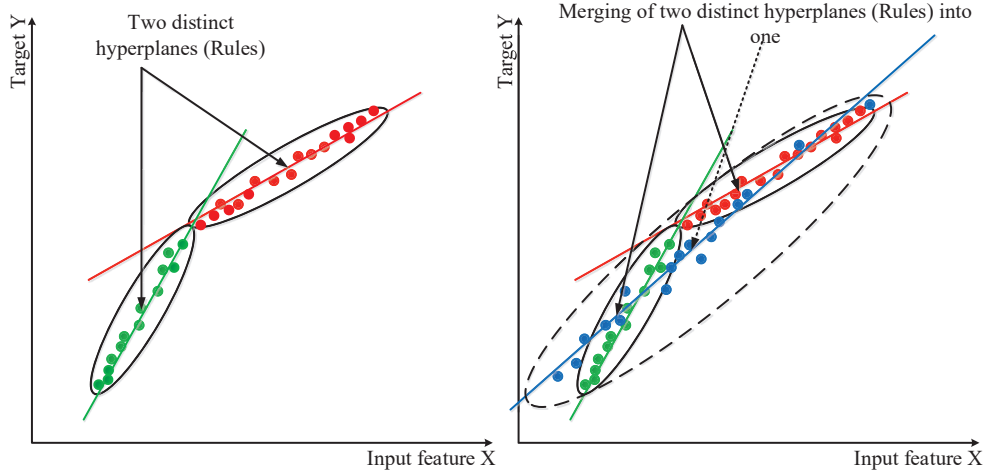


Figure 2. Merging of redundant hyperplanes (rules) due to newly incoming training samples

where no addition of rules occurs. This strategy aims to attain a stable rule evolution and prevents new rules to be merged straightaway after being introduced in the rule base. As an alternative, the Yager's participatory learning-inspired merging scenario [45] can be used to merge the two hyperplanes.

C. Adaptation of Hyperplanes

In previous work on hyperplane based T-S fuzzy system [48], recursive least square (RLS) method is employed to calculate parameters of hyperplane. As an advancement to the RLS method, a term for decaying the consequent parameter in the cost function of the RLS method is utilized in [49] and helps to obtain a solid generalization performance - generalized recursive least square (GRLS) approach. However, their approach is formed in the context of global learning. A local learning method has some advantages over its global counterpart: interpretability and robustness over noise. The interpretability is supported by the fact that each hyperplane portrays specific operating region of approximation curve. Also, in local learning, the generation or deletion of any rule does not harm the convergence of the consequent parameters of other rules, which results in a significantly stable updating process [50].

Due to the desired features of local learning scenario, the GRLS method is extended in [9], [11]: Fuzzily Weighted Generalised Recursive Least Square (FWGRLS) method. FWGRLS can be seen also as a variation of Fuzzily Weighted Recursive Least Square (FWRLS) method [7] with insertion of weight decay term. The FWGRLS method is formed in the proposed type-1 PALM, where the cost function can be expressed as:

$$J_{L_j}^n = (y_t - x_e \pi_j) \Lambda_j (y_t - x_e \pi_j) + 2\beta \varphi(\pi_j) + (\pi - \pi_j) (C_j x_e)^{-1} (\pi - \pi_j) \quad (27)$$

$$J_L^n = \sum_{j=1}^i J_{L_j}^n \quad (28)$$

where Λ_j denotes a diagonal matrix with the diagonal element of R_j , β represents a regularization parameter, φ is a decaying factor, x_e is the extended input vector, C_j is the covariance matrix, π_j is the local subsystem of the j th hyperplane. Following the similar approach as [9], the final expression of the FWGRLS approach is formed as follows:

$$\pi_j(k) = \pi_j(k-1) - \beta C_j(k) \nabla \varphi \pi_j(k-1) + \Upsilon(k) (y_t(k) - x_e \pi_j(k)); \quad j = [1, 2, \dots, R] \quad (29)$$

where

$$C_j(k) = C_j(k-1) - \Upsilon(k) x_e C_j(k-1) \quad (30)$$

$$\Upsilon(k) = C_j(k-1) x_e \left(\frac{1}{\Lambda_j} + x_e C_j(k-1) x_e^T \right)^{-1} \quad (31)$$

with the initial conditions

$$\pi_1(1) = 0 \quad \text{and} \quad C_1(1) = \Omega I \quad (32)$$

where $\Upsilon(k)$ denotes the Kalman gain, R is the number of rules, $\Omega = 10^5$ is a large positive constant. In this work, the regularization parameter β is assigned as an extremely small value ($\beta \approx 10^{-7}$). It can be observed that the FWGRLS method is similar to the RLS method without the term $\beta \pi_j(k) \nabla \varphi(k)$. This term steers the value of $\pi_j(k)$ even to update an insignificant amount of it minimizing the impact of inconsequential rules. The quadratic weight decay function is chosen in PALM written as follows:

$$\varphi(\pi_j(k-1)) = \frac{1}{2} (\pi_j(k-1))^2 \quad (33)$$

Its gradient can be expressed as:

$$\nabla \varphi(\pi_j(k-1)) = \pi_j(k-1) \quad (34)$$

By utilizing this function, the adapted-weight is shrunk to a factor proportional to the present value. It helps to intensify

the generalization capability by maintaining dynamic of output weights into small values [51].

V. ONLINE LEARNING POLICY IN TYPE-2 PALM

The learning policy of the type-1 PALM is extended in the context of the type-2 fuzzy system, where q design factor is utilized to carry out the type-reduction scenario. The learning mechanisms are detailed in the following subsections.

A. Mechanism of Growing Rules

In realm of the type-2 fuzzy system, the SSC method has been extended to the type-2 SSC (T2SSC) in [17]. It has been adopted and extended in terms of the design factors q_l and q_r , since the original work in [17] only deals with a single design factor q . In this T2SSC method, the rule significance is measured by calculating the input and output coherence as done in the type-1 system. By assuming $\tilde{\mathcal{H}}_i = [\overline{\mathcal{H}}_i, \underline{\mathcal{H}}_i] \in \mathfrak{R}^{R \times (1+n)}$ as interval-valued hyperplane of the i th local sub-model, the input and output coherence for our proposed type-2 system can be extended as follows:

$$I_{c_L}(\tilde{\mathcal{H}}_i, X_t) = (1 - q_l)\xi(\overline{\mathcal{H}}_i, X_t) + q_l\xi(\underline{\mathcal{H}}_i, X_t) \quad (35)$$

$$I_{c_R}(\tilde{\mathcal{H}}_i, X_t) = (1 - q_r)\xi(\overline{\mathcal{H}}_i, X_t) + q_r\xi(\underline{\mathcal{H}}_i, X_t) \quad (36)$$

$$I_c(\tilde{\mathcal{H}}_i, X_t) = \frac{(I_{c_L}(\tilde{\mathcal{H}}_i, X_t) + I_{c_R}(\tilde{\mathcal{H}}_i, X_t))}{2} \quad (37)$$

$$O_c(\tilde{\mathcal{H}}_i, X_t) = \xi(X_t, T_t) - \xi(\tilde{\mathcal{H}}_i, T_t) \quad (38)$$

where

$$\xi_L(\tilde{\mathcal{H}}_i, T_t) = (1 - q_l)\xi(\overline{\mathcal{H}}_i, T_t) + q_l\xi(\underline{\mathcal{H}}_i, T_t) \quad (39)$$

$$\xi_R(\tilde{\mathcal{H}}_i, T_t) = (1 - q_r)\xi(\overline{\mathcal{H}}_i, T_t) + q_r\xi(\underline{\mathcal{H}}_i, T_t) \quad (40)$$

$$\xi(\tilde{\mathcal{H}}_i, T_t) = \frac{(\xi_L(\tilde{\mathcal{H}}_i, T_t) + \xi_R(\tilde{\mathcal{H}}_i, T_t))}{2} \quad (41)$$

Unlike the direct calculation of input coherence $I_c(\cdot)$ in type-1 system, in type-2 system the $I_c(\cdot)$ is calculated using (37) based on left $I_{c_L}(\cdot)$ and right $I_{c_R}(\cdot)$ input coherence. By using the MCI method in the T2SSC rule growing process, the correlation is measured using (18) and (19), where (X_t, T_t) are substituted with $(\overline{\mathcal{H}}_i, X_t)$, $(\underline{\mathcal{H}}_i, X_t)$, $(\overline{\mathcal{H}}_i, T_t)$, $(\underline{\mathcal{H}}_i, T_t)$. The conditions for growing rules remain the same as expressed in (20) and is only modified to fit the type-2 fuzzy system platform. The parameter settings for the predefined thresholds are as with the type-1 fuzzy model.

B. Mechanism of Merging Rules

The merging mechanism of the type-1 PALM is extended for the type-2 fuzzy model. To merge the rules, both the angle and distance between two interval-valued hyperplanes are measured as follows:

$$\tilde{\theta}_{hp} = \arccos\left(\left|\frac{\tilde{\omega}_R^T \tilde{\omega}_{R+1}}{|\tilde{\omega}_R| |\tilde{\omega}_{R+1}|}\right|\right) \quad (42)$$

$$\tilde{d}_{R,R+1} = \left|(\tilde{a}_1 - \tilde{a}_2) \cdot \frac{(\tilde{b}_1 \times \tilde{b}_2)}{|\tilde{b}_1 \times \tilde{b}_2|}\right| \quad (43)$$

where $\tilde{\theta}_{hp} = [\underline{\theta}_{hp}, \overline{\theta}_{hp}]$, and $\tilde{d}_{R,R+1} = [\underline{d}_{R,R+1}, \overline{d}_{R,R+1}]$. This $\tilde{\theta}_{hp}$ and $\tilde{d}_{R,R+1}$ also needs to satisfy the condition of (24) to merge the rules, where the same range of c_1 and c_2 are applied in the type-2 PALM. The formula of merged weight in (25) is extended for the interval-valued merged weight as follows:

$$\tilde{\omega}_{acm}^{new} = \frac{\tilde{\omega}_{acm}^{old} N_{acm}^{old} + \tilde{\omega}_{acm+1}^{old} N_{acm+1}^{old}}{N_{acm}^{old} + N_{acm+1}^{old}} \quad (44)$$

where $\tilde{\omega}_{acm} = [\underline{\omega}_{acm}, \overline{\omega}_{acm}]$. As with the type-1 PALM, the weighted average strategy is followed in the rule merging procedure of the type-2 PALM.

C. Learning of the Hyperplane Submodels Parameters

The FWGRLS method [9] is extended to adjust the upper and lower hyperplanes of the interval type-2 PALM. The final expression of the FWGRLS method is shown as follows:

$$\begin{aligned} \tilde{\pi}_j(k) &= \tilde{\pi}_j(k-1) - \beta \tilde{C}_j(k) \nabla \varphi \tilde{\pi}_j(k-1) + \\ &\tilde{\Upsilon}(k)(y_t(k) - x_e \tilde{\pi}_j(k)); \quad j = [1, 2, \dots, R] \end{aligned} \quad (45)$$

where

$$\tilde{C}_j(k) = \tilde{C}_j(k-1) - \tilde{\Upsilon}(k) x_e \tilde{C}_j(k-1) \quad (46)$$

$$\tilde{\Upsilon}(k) = \tilde{C}_j(k-1) x_e \left(\frac{1}{\tilde{\Lambda}_j} + x_e \tilde{C}_j(k-1) x_e^T \right)^{-1} \quad (47)$$

where $\tilde{\pi}_j = [\underline{\pi}_j, \overline{\pi}_j]$, $\tilde{C}_j = [\underline{C}_j, \overline{C}_j]$, $\tilde{\Upsilon} = [\underline{\Upsilon}, \overline{\Upsilon}]$, and $\tilde{\Lambda}_j = [\underline{\Lambda}_j, \overline{\Lambda}_j]$. The quadratic weight decay function of FWGRLS method remains in the type-2 PALM to provide the weight decay effect in the rule merging scenario.

D. Adaptation of q Design Factors

The q design factor as used in [11] is extended in terms of left q_l and right q_r design factor to actualize a high degree of freedom of the type-2 fuzzy model. They are initialized in such a way that the condition $q_r > q_l$ is maintained. In this adaptation process, the gradient of q_l and q_r with respect to error $E = \frac{1}{2}(y_d - y_{out})^2$ can be expressed as follows:

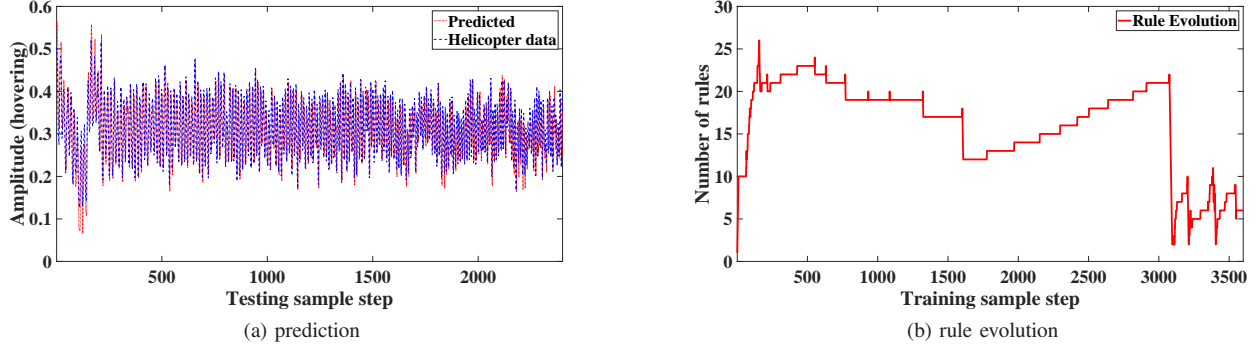


Figure 3. (a) Online identification of helicopter (in hovering condition); (b) rule evolution in that identification using type-2 PALM (L)

$$\begin{aligned} \frac{\partial E}{\partial q_l} &= \frac{\partial E}{\partial y_{out}} \times \frac{\partial y_{out}}{\partial y_{l_{out}}} \times \frac{\partial y_{l_{out}}}{\partial q_l} \\ &= -\frac{1}{2} (y_d - y_{out}) \left(\frac{f_{out}^1 f_{out}^2}{\sum_{i=1}^R \bar{f}_{out}^1} - \frac{\bar{f}_{out}^1 f_{out}^2}{\sum_{i=1}^R f_{out}^1} \right) \end{aligned} \quad (48)$$

$$\begin{aligned} \frac{\partial E}{\partial q_r} &= \frac{\partial E}{\partial y_{out}} \times \frac{\partial y_{out}}{\partial y_{r_{out}}} \times \frac{\partial y_{r_{out}}}{\partial q_r} \\ &= -\frac{1}{2} (y_d - y_{out}) \left(\frac{f_{out}^1 \bar{f}_{out}^2}{\sum_{i=1}^R \bar{f}_{out}^1} - \frac{\bar{f}_{out}^1 \bar{f}_{out}^2}{\sum_{i=1}^R f_{out}^1} \right) \end{aligned} \quad (49)$$

After obtaining the gradient $\frac{\partial E}{\partial q_l}$ and $\frac{\partial E}{\partial q_r}$, the q_l and q_r are updated using formulas as follows:

$$q_l^{new} = q_l^{old} - a \frac{\partial E}{\partial q_l^{old}} \quad (50)$$

$$q_r^{new} = q_r^{old} - a \frac{\partial E}{\partial q_r^{old}} \quad (51)$$

where $a = 0.1$ is a learning rate. Note that the learning rate is a key of q_l and q_r convergence because it determines the step size of adjustment. An adaptive strategy as done in [38] can be implemented to shorten the convergence time without compromising the stability of adaptation process.

E. Impediments of the Basic PALM structure

In the PALM, hyperplane-shaped membership function is formulated exercising a distance ($dst(j)$) exposed in (5). The ($dst(j)$) is calculated using true output value based on theory of point to hyperplane distance [25]. Therefore, the PALM has a dependency on the true output in deployment phase. Usually, true outputs are not known in the deployment mode. To circumvent such structural shortcoming, the so-called "Teacher Forcing" mechanism [52] is employed in PALM. In teacher forcing technique, network has connections from outputs to their hidden nodes at the next time step. Based on this concept, the output of PALM is connected with the input layer at the next step, which constructs a recurrent PALM (RPALM) architecture. The modified distance formula for the RPALM

architecture is provided in the supplementary document. Besides, the code of the proposed RPALM is made available in [53]. Our numerical results demonstrate that rPALM produces minor decrease of predictive accuracy compared to PALM but is still better than many of benchmarked SANFSSs. The downside of the RPALM is that the rules are slightly not transparent because it relies on its predicted output of the previous time instant $y(k-1)$ rather than incoming input x_k .

VI. EVALUATION

PALM has been evaluated through numerical studies with the use of synthetic and real-world streaming datasets. The code of PALMs and RPALMs along with these datasets have been made publicly available in [26], [53].

A. Experimental Setup

1) *Synthetic Streaming Datasets*: Three synthetic streaming datasets are utilized in our work to evaluate the adaptive mechanism of the PALM: 1) Box-Jenkins Time Series dataset; 2) the Mackey-Glass Chaotic Time Series dataset; and 3) non-linear system identification dataset.

a) *Box-Jenkins Gas Furnace Time Series Dataset*: The Box-Jenkins (BJ) gas furnace dataset is a famous benchmark problem in the literature to verify the performance of SANFSSs. The objective of the BJ gas furnace problem is to model the output ($y(k)$) i.e. the CO_2 concentration from the time-delayed input ($u(k-4)$) methane flow rate and its previous output $y(k-1)$. The I/O configuration follows the standard setting in the literature as follows:

$$\hat{y}(k) = f(u(k-4), y(k-1)) \quad (52)$$

This problem consists of 290 data samples (52) where 200 samples are reserved for the training samples while remaining 90 samples are used to test model's generalization.

b) *Mackey-Glass Chaotic Time Series Dataset*: Mackey-Glass (MG) chaotic time series problem having its root in [56] is a popular benchmark problem to forecast the future value of a chaotic differential delay equation by using the past values. Many researchers have used the MG dataset to evaluate their SANFSSs' learning and generalization performance.

Table I
MODELING OF THE BOX-JENKINS TIME SERIES USING VARIOUS SELF-ADAPTIVE NEURO-FUZZY SYSTEMS

Model	Reference	RMSE using testing samples	NDEI using testing samples	Number of rules	Number of inputs	Network Parameters	Number of training samples	Execution time (sec)
DFNN	[41]	0.7800	4.8619	1	2	6	200	0.0933
GDFNN	[54]	0.0617	0.3843	1	2	7	200	0.0964
FAOSPFNN	[55]	0.0716	0.4466	1	2	4	200	0.0897
eTS	[7]	0.0604	0.3763	5	2	30	200	0.0635
simp_eTS	[8]	0.0607	0.3782	3	2	18	200	1.5255
GENEFIS	[9]	0.0479	0.2988	2	2	18	200	0.0925
PANFIS	[10]	0.0672	0.4191	2	2	18	200	0.3162
pRVFLN	[17]	0.0478	0.2984	2	2	10	200	0.0614
Type-1 PALM (L)	-	0.0484	0.3019	8	2	24	200	0.1972
Type-1 PALM (G)	-	0.0439	0.2739	8	2	24	200	0.1244
Type-2 PALM (L)	-	0.0377	0.2355	2	2	12	200	0.2723
Type-2 PALM (G)	-	0.0066	0.0410	14	2	84	200	0.3558

This dataset is characterized by their nonlinear and chaotic behaviors where its nonlinear oscillations replicate most of the physiological processes. The MG dataset is initially proposed as a control model of the generation of white blood cells. The mathematical model is expressed as:

$$\frac{dy(k)}{dt} = \frac{by(k - \delta)}{1 + y^{10}y(k - \delta)} - ay(k) \quad (53)$$

where $b = 0.2$, $a = 0.1$, and $\delta = 85$. The chaotic element is primarily attributed by $\delta \geq 17$. Data samples are generated through the fourth-order Range Kutta method and our goal is to predict the system output $\hat{y}(k + 85)$ at $k = 85$ using four inputs: $y(k)$, $y(k - 6)$, $y(k - 12)$, and $y(k - 18)$. This series-parallel regression model can be expressed as follows:

$$\hat{y}(k + 85) = f(y(k), y(k - 6), y(k - 12), y(k - 18)) \quad (54)$$

For the training purpose, a total of 3000 samples between $k = 201$ and $k = 3200$ is generated with the help of the 4th-order Range-Kutta method, whereas the predictive model is tested with unseen 500 samples in the range of $k = 5001 - 5500$ to assess the generalization capability of the PALM.

c) Non-linear System Identification Dataset: A non-linear system identification is put forward to validate the efficacy of PALM and has frequently been used by researchers to test their SANFSS. The nonlinear dynamic of the system can be formulated by the following differential equation:

$$y(k + 1) = \frac{y(k)}{1 + y^2(k)} + u^3(k) \quad (55)$$

where $u(k) = \sin(2\pi k/100)$. The predicted output of the system $\hat{y}(k + 1)$ depends on the previous inputs and its own lagged outputs, which can be expressed as follows:

$$\hat{y}(k + 1) = f(y(k), y(k - 1), \dots, y(k - 10), u(k)) \quad (56)$$

The first 50000 samples are employed to build our predictive model, and other 200 samples are fed the model to test model's generalization.

2) Real-World Streaming Datasets: Three different real-world streaming datasets from two rotary wing unmanned aerial vehicle's (RUAV) experimental flight tests and a time-varying stock index forecasting data are exploited to study the performance of PALM.

a) Quadcopter Unmanned Aerial Vehicle Streaming Data: A real-world streaming dataset is collected from a Pixhawk autopilot framework based quadcopter RUAV's experimental flight test. All experiments are performed in the indoor UAV laboratory at the University of New South Wales, Canberra campus. To record quadcopter flight data, the Robot Operating System (ROS), running under the Ubuntu 16.04 version of Linux is used. By using the ROS, a well-structured communication layer is introduced into the quadcopter reducing the burden of having to reinvent necessary software.

During the real-time flight testing accurate vehicle position, velocity, and orientation are the required information to identify the quadcopter online. For system identification, a flight data of quadcopter's altitude containing approximately 9000 samples are recorded with some noise from VICON optical motion capture system. Among them, 60% of the samples are used for training and remaining 40% are for testing. In this work, our model's output $y(k)$ is estimated as $\hat{y}(k)$ from the previous point $y(k-6)$, and the system input $u(k)$, which is the required thrust to the rotors of the quadcopter. The regression model from the quadcopter data stream can be expressed as follows:

$$\hat{y}(k) = f(y(k - 6), u(k)) \quad (57)$$

b) Helicopter Unmanned Aerial Vehicle Streaming Data: The chosen RUAV for gathering streaming dataset is a Taiwanese made Align Trex450 Pro Direct Flight Control (DFC), fly bar-less, helicopter. The high degree of non-linearity associated with the Trex450 RUAV vertical dynamics makes it challenging to build a regression model from experimental data streams. All experiments are conducted at the UAV laboratory of the UNSW Canberra campus. Flight data consists of 6000 samples collected in near hover, heave and in ground effect flight conditions to simulate non-stationary environments. First 3600 samples are used for the training data, and the rest of the data are aimed to test the model. The nonlinear dependence

of the helicopter RUAV is governed by the regression model as follows:

$$\hat{y}(k+1) = f(y(k), u(k)) \quad (58)$$

where $\hat{y}(k+1)$ is the estimated output of the helicopter system at $k = 1$.

c) *Time-Varying Stock Index Forecasting Data*: Our proposed PALM has been evaluated by the time-varying dataset, namely the prediction of Standard and Poor's 500 (S&P-500 (^GSPC)) market index [57], [58]. The dataset consists of sixty years of daily index values ranging from 3 January 1950 to 12 March 2009, downloaded from [59]. This problem comprises 14893 data samples. In our work, the reversed order data points of the same 60 years indexes have amalgamated with the original dataset, forming a new dataset with 29786 index values. Among them, 14893 samples are allocated to train the model and the remainder of 14893 samples are used for the validation data. The target variable is the next day S&P-500 index $y(k+1)$ predicted using previous five consecutive days indexes: $y(k)$, $y(k-1)$, $y(k-2)$, $y(k-3)$ and $y(k-4)$. The functional relationship of the predictive model is formalized as follows:

$$\hat{y}(k+1) = f(y(k), y(k-1), y(k-2), y(k-3), y(k-4)) \quad (59)$$

This dataset carries the sudden drift property which happens around 2008. This property corresponds to the economic recession in the US due to the housing crisis in 2009.

B. Results and Discussion

In this work, we have developed PALM by implementing type-1 and type-2 fuzzy concept, where both of them are simulated under two parameter optimization scenarios: 1) Type-1 PALM (L); 2) Type-1 PALM (G); 3) Type-2 PALM (L); 4) Type-2 PALM (G). *L* denotes the *Local* update strategy while *G* stands for the *Global* learning mechanism. Basic PALM models are tested with three synthetic and three real-world streaming datasets. Furthermore, the models are compared against eight prominent variants of SANFSSs, namely DFNN [41], GDFNN [54], FAOSPFNN [55], eTS [7], simp_eTS [8], GENEFIS [9], PANFIS [10], and pRVFLN [17]. Experiments with real-world and synthesis data streams are repeated with recurrent PALM. All experimental results using the RPALM are also purveyed in the supplementary document. Proposed PALMs' efficacy has been evaluated by measuring the root mean square error (RMSE), and nondimensional error index (NDEI) written as follows:

$$MSE = \frac{\sum_{k=1}^N (y_t - y_k)^2}{N_{T_s}}, \quad RMSE = \sqrt{MSE} \quad (60)$$

$$NDEI = \frac{RMSE}{Std(T_s)} \quad (61)$$

where N_{T_s} is the total number of testing samples, and $Std(T_s)$ denotes a standard deviation over all actual output values in

the testing set. A comparison is produced under the same computational platform in Intel(R) Xeon(R) E5-1630 v4 CPU with a 3.70 GHz processor and 16.0 GB installed memory.

1) Results and Discussion on Synthetic Streaming Datasets:

Table I sums up the outcomes of the Box-Jenkins time series for all benchmarked models. Among various models, our proposed type-2 PALM (G) clearly outperforms other consolidated algorithms in terms of predictive accuracy. For instance, the measured NDEI is just 0.0598 - the lowest among all models. Type-2 PALM (G) generates thirteen (13) rules to achieve this accuracy level. Although the number of generated rules is higher than that of remaining models, this accuracy far exceeds its counterparts whose accuracy hovers around 0.29. A fair comparison is also established by utilizing very close number of rules in some benchmarked strategies namely eTS, simp_eTS, PANFIS, and GENEFIS. By doing so the lowest observed NDEI among the benchmarked variations is 0.29, delivered by GENEFIS. It is substantially higher than the measured NDEI of type-2 PALM (G). The advantage of HPBC is evidenced by the number of PALM's network parameters, where with thirteen rules and two inputs, PALM evolves only 39 parameters, whereas the number of network parameters of other algorithm for instance GENEFIS is 117. PALM requires the fewest parameters than all the other variants of SANFSS as well and affects positively to execution speed of PALM. On the other hand, with only one rule the NDEI of PALM is also lower than the benchmarked variants as observed in type-2 PALM (L) from Table I, where it requires only 3 network parameter. It is important to note that the rule merging mechanism is active in the case of only local learning scenario. Here the number of induced rules are 8 and 2, which is lower than i.e. 8 and 14 in their global learning versions. In both cases of G and L, the NDEI is very close to each other with a very similar number of rules. In short, PALM constructs a compact regression model using the Box-Jenkins time series with the least number of network parameters while producing the most reliable prediction.

The prediction of Mackey–Glass chaotic time series is challenging due to the nonlinear and chaotic behavior. Numerical results on the Mackey–Glass chaotic time series dataset is consolidated in Table II, where 500 unseen samples are used to test all the models. Due to the highly nonlinear behavior, an NDEI lower than 0.2 was obtained from only GENEFIS [9] among other benchmarked algorithms. However, it costs 42 rules and requires a big number (1050) of network parameters. On the contrary, with only 13 rules, 65 network parameters and faster execution, the type-2 PALM (G) attains NDEI of 0.0685, where this result is traced within 2.45 seconds due to the deployment of fewer parameters than its counterparts. The use of rule merging method in local learning mode reduces the generated rules to five (5) - type-1 PALM (L). A comparable accuracy is obtained from type-1 PALM (L) with only 5 rules and 25 network parameters. An accomplishment of such accuracy with few parameters decreases the compu-

Table II
MODELING OF THE MACKEY–GLASS CHAOTIC TIME SERIES USING VARIOUS SELF-ADAPTIVE NEURO-FUZZY SYSTEMS

Model	Reference	RMSE using testing samples	NDEI using testing samples	Number of rules	Number of inputs	Network Parameters	Number of training samples	Execution time (sec)
DFNN	[41]	3.0531	12.0463	1	4	10	3000	11.1674
GDFNN	[54]	0.1520	0.6030	1	4	13	3000	12.1076
FAOSPFNN	[55]	0.2360	0.9314	1	4	6	3000	13.2213
eTS	[7]	0.0734	0.2899	48	4	480	3000	8.6174
simp_eTS	[8]	0.0623	0.2461	75	4	750	3000	20.9274
GENEFIS	[9]	0.0303	0.1198	42	4	1050	3000	4.9694
PANFIS	[10]	0.0721	0.2847	33	4	825	3000	4.8679
pRVFLN	[17]	0.1168	0.4615	2	4	18	2993	0.9236
Type-1 PALM (L)	-	0.0688	0.2718	5	4	25	3000	0.8316
Type-1 PALM (G)	-	0.0349	0.1380	18	4	90	3000	0.7771
Type-2 PALM (L)	-	0.0444	0.1755	11	4	110	3000	2.8138
Type-2 PALM (G)	-	0.0159	0.0685	13	4	130	3000	2.4502

Table III
MODELING OF THE NON-LINEAR SYSTEM USING VARIOUS SELF-ADAPTIVE NEURO-FUZZY SYSTEMS

Model	Reference	RMSE using testing samples	NDEI using testing samples	Number of rules	Number of inputs	Network Parameters	Number of training samples	Execution time (sec)
DFNN	[41]	0.0380	0.0404	2	2	12	50000	2149.246
GDFNN	[54]	0.0440	0.0468	2	2	14	50000	2355.726
FAOSPFNN	[55]	0.0027	0.0029	4	2	16	50000	387.7890
eTS	[7]	0.07570	0.08054	7	2	42	50000	108.5791
simp_eTS	[8]	0.07417	0.07892	7	2	42	50000	129.5552
GENEFIS	[9]	0.00041	0.00043	6	2	54	50000	10.9021
PANFIS	[10]	0.00264	0.00281	27	2	243	50000	42.4945
pRVFLN	[17]	0.06395	0.06596	2	2	10	49999	12.0105
Type-1 PALM (L)	-	0.08808	0.09371	5	2	15	50000	9.9177
Type-1 PALM (G)	-	0.07457	0.07804	9	2	27	50000	10.5712
Type-2 PALM (L)	-	0.03277	0.03487	3	2	18	50000	13.7455
Type-2 PALM (G)	-	0.00387	0.00412	21	2	126	50000	55.4865

tational complexity in predicting complex nonlinear system as witnessed from type-1 PALM (L) in Table II. Due to low computational burden, the lowest execution time of 0.7771 seconds is achieved by the type-1 PALM (G).

PALM has been utilized to estimate a high-dimensional nonlinear system with 50000 training samples. this study case depicts similar trend where PALM is capable of delivering comparable accuracy but with much less computational complexity and memory demand. The deployment of rule merging module lessens the number of rules from 9 to 5 in case of type-1 PALM, and 3 from 21 in type-2 PALM. The obtained NDEI of PALMs with such a small number of rules is also similar to other SANFS variants. To sum up, the PALM can deal with streaming examples with low computational burden due to the utilization of few network parameters, where it maintains a comparable or better predictive accuracy.

2) Results and Discussion on Real-World Data Streams:

Table IV outlines the results of online identification of a quadcopter RUAV from experimental flight test data. A total 9112 samples of quadcopter's hovering test with a very high noise from motion capture technique namely VICON [60] is recorded. Building SANFS using the noisy streaming dataset is computationally expensive as seen from a high execution time of the benchmarked SANFSs. Contrast with these standard SANFSs, a quick execution time is seen from PALMs. It

happens due to the requirement of few network parameters. Besides, PALM arrives at encouraging accuracy as well. For instance, the lowest NDEI at just 0.1538 is elicited in type-2 PALM (G). To put it plainly, due to utilizing incremental HPBC, PALM can perform better than its counterparts SANFSs driven by HSSC and HESC methods when dealing with noisy datasets.

The online identification of a helicopter RUAV (Trex450 Pro) from experimental flight data at hovering condition are tabulated in Table V. The highest identification accuracy with the NDEI of only 0.1380 is obtained from the proposed type-2 PALM (G) with 9 rules. As with the previous experiments, the activation of rule merging scenario reduces the fuzzy rules significantly from 11 to 6 in type-1 PALM, and from 9 to 6 in type-2 PALM. The highest accuracy is produced by type-2 PALM with only 4 rules due to most likely uncertainty handling capacity of type-2 fuzzy system. PALM's prediction on the helicopter's hovering dynamic and its rule evolution are depicted in Fig. 3. These figures are produced by the type-2 PALM(L). For further clarification, the fuzzy rule extracted by type-1 PALM(L) in case of modeling helicopter can be uttered

Table IV
ONLINE MODELING OF THE QUADCOPTER UTILIZING VARIOUS SELF-ADAPTIVE NEURO-FUZZY SYSTEMS

Model	Reference	RMSE using testing samples	NDEI using testing samples	Number of rules	Number of inputs	Network Parameters	Number of training samples	Execution time (sec)
DFNN	[41]	0.1469	0.6925	1	2	6	5467	19.0962
GDFNN	[54]	0.1442	0.6800	1	2	7	5467	20.1737
FAOSPFNN	[55]	0.2141	1.0097	12	2	48	5467	25.4000
eTS	[7]	0.1361	0.6417	4	2	24	5467	3.0686
simp_eTS	[8]	0.1282	0.6048	4	2	24	5467	3.9984
GENEFIS	[9]	0.1327	0.6257	1	2	9	5467	1.7368
PANFIS	[10]	0.1925	0.9077	47	2	424	5467	6.0244
pRVFLN	[17]	0.1191	0.5223	1	2	5	5461	0.9485
Type-1 PALM (L)	-	0.1311	0.6182	2	2	6	5467	0.6605
Type-1 PALM (G)	-	0.1122	0.5290	2	2	6	5467	0.5161
Type-2 PALM (L)	-	0.1001	0.4723	3	2	18	5467	1.7049
Type-2 PALM (G)	-	0.0326	0.1538	4	2	24	5467	1.6802

as follows:

$$R^1 : \text{IF } X \text{ is close to } \left([1, x_1, x_2] \times [0.0186, -0.0909, 0.9997]^T \right), \text{ THEN } y_1 = 0.0186 - 0.0909x_1 + 0.9997x_2 \quad (62)$$

In (62), the antecedent part is manifesting the hyperplane. The consequent part is simply $y_1 = x_e^1 \omega$, where $\omega \in \mathbb{R}^{(n+1) \times 1}$, n is the number of input dimension. Usage of 2 inputs in the experiment of Table V assembles an extended input vector like: $x_e^1 = [1, x_1, x_2]$. The weight vector is: $[\omega_{01}, \omega_{11}, \omega_{21}] = [0.3334, 0.3334, 0.3334]$ In case of Type-2 local learning configuration, a rule can be stated as follows:

$$R^1 : \text{IF } X \text{ is close to } \left(([1, x_1, x_2] \times [0.0787, -0.3179, 1.0281]^T), ([1, x_1, x_2] \times [0.2587, -0.1767, 1.2042]^T) \right) \quad (63)$$

$$\text{THEN } y_1 = [0.0787, 0.2587] + [-0.3179, -0.1767]x_1 + [1.0281, 1.2042]x_2$$

where (63) is expressing the first rule among 6 rules formed in that experiment in Type-2 PALM's local learning scenario. Since the PALM has no premise parameters, the antecedent part is just presenting the interval-valued hyperplanes. The consequent part is noting but $y_1 = x_e^1 \tilde{\omega}$, where $\tilde{\omega} \in \mathbb{R}^{(2(n+1)) \times 1}$, n is the number of input dimension. Since 2 inputs are available in the experiment of Table V, the extended input vector is: $x_e^1 = [1, x_1, x_2]$, and interval-valued weight vectors are: $[\omega_{01}, \bar{\omega}_{01}] = [0.0787, 0.2587]$; $[\omega_{11}, \bar{\omega}_{11}] = [-0.3179, -0.1767]$; $[\omega_{21}, \bar{\omega}_{21}] = [1.0281, 1.2042]$. Furthermore, the predictive capability, rule evolution, NDEI evolution and error of the PALM for six streaming datasets are attached in the supplementary document to keep the paper compact.

The numerical results on the time-varying Stock Index Forecasting S&P-500 (^GSPC) problem are organized in Table VI. The lowest number of network parameters is obtained from PALMs, and subsequently, the fastest training speed of 2.0326 seconds is attained by type-1 PALM (L). All consolidated

benchmarked algorithms generate the same level of accuracy around 0.015 to 0.06.

C. Sensitivity Analysis of Predefined Thresholds

In the rule growing purpose, two predefined thresholds (b_1 and b_2) are utilized in our work. During various experimentation, it has been observed that the higher the value of b_1 , the less the number of hyperplanes are added and vice versa. Unlike the effect of b_1 , in case of b_2 , at higher values, more hyperplanes are added and vice versa. To further validate this feature, the sensitivity of b_1 and b_2 is evaluated using the Box-Jenkins (BJ) gas furnace dataset. The same I/O relationship as described in the subsection VI-A is applied here, where the model is trained also with same 200 samples and remaining 90 unseen samples are used to test the model.

In the first test, b_2 is varied in the range of $[0.052, 0.053, 0.054, 0.055]$, while the value of b_1 is kept fixed at 0.020. On the other hand, the varied range for b_1 is $[0.020, 0.022, 0.024, 0.026]$, while b_2 is maintained at 0.055. In the second test, the altering range for b_1 is $[0.031, 0.033, 0.035, 0.037]$, and for b_2 is $[0.044, 0.046, 0.048, 0.050]$. In this test, for a varying b_1 , the constant value of b_2 is 0.050, where b_1 is fixed at 0.035 during the change of b_2 . To evaluate the sensitivity of these thresholds, normalized RMSE (NRMSE), NDEI, running time, and number of rules are reported in Table VII. The NRMSE formula can be expressed as:

$$NRMSE = \sqrt{\frac{MSE}{Std(T_s)}} \quad (64)$$

From Table VII, it has been observed that in the first test for different values of b_1 and b_2 , the value of NRMSE and NDEI remains stable at 0.023 and 0.059 respectively. The execution time varies in a stable range of $[0.31, 0.35]$ seconds and the number of generated rules is 13. In the second test, the NRMSE, NDEI, and execution time are relatively constant in the range of $[0.046, 0.048]$, $[0.115, 0.121]$,

Table V
ONLINE MODELING OF THE HELICOPTER UTILIZING VARIOUS SELF-ADAPTIVE NEURO-FUZZY SYSTEMS

Model	Reference	RMSE using testing samples	NDEI using testing samples	Number of rules	Number of inputs	Network Parameters	Number of training samples	Execution time (sec)
DFNN	[41]	0.0426	0.6644	1	2	6	3600	8.7760
GDFNN	[54]	0.0326	0.5082	2	2	14	3600	11.2705
FAOSPFNN	[55]	0.0368	0.5733	2	2	8	3600	2.4266
eTS	[7]	0.0535	0.8352	3	2	18	3600	1.3822
simp_eTS	[8]	0.0534	0.8336	3	2	18	3600	2.3144
GENEFIS	[9]	0.0355	0.5541	2	2	18	3600	0.6736
PANFIS	[10]	0.0362	0.5652	9	2	81	3600	1.4571
pRVFLN	[17]	0.0329	0.5137	2	2	10	3362	1.0195
Type-1 PALM (L)	-	0.0363	0.5668	6	2	18	3600	0.9789
Type-1 PALM (G)	-	0.0313	0.4886	11	2	33	3600	0.9517
Type-2 PALM (L)	-	0.0201	0.3141	6	2	36	3600	2.3187
Type-2 PALM (G)	-	0.0088	0.1380	9	2	54	3600	1.9496

Table VI
MODELING OF THE TIME-VARYING STOCK INDEX FORECASTING USING VARIOUS SELF-ADAPTIVE NEURO-FUZZY SYSTEMS

Model	Reference	RMSE using testing samples	NDEI using testing samples	Number of rules	Number of inputs	Network Parameters	Number of training samples	Execution time (sec)
DFNN	[41]	0.00441	0.01554	1	5	12	14893	347.7522
GDFNN	[54]	0.30363	1.07075	1	5	16	14893	344.4558
FAOSPFNN	[55]	0.20232	0.71346	1	5	7	14893	15.1439
eTS	[7]	0.01879	0.06629	3	5	36	14893	30.1606
simp_eTS	[8]	0.00602	0.02124	3	5	36	14893	29.4296
GENEFIS	[9]	0.00849	0.02994	3	5	108	14893	2.2076
PANFIS	[10]	0.00464	0.01637	8	5	288	14893	5.2529
pRVFLN	[17]	0.00441	0.01555	1	5	11	11170	2.5104
Type-1 PALM (L)	-	0.00273	0.00964	3	5	18	14893	2.0326
Type-1 PALM (G)	-	0.00235	0.00832	5	5	30	14893	2.2802
Type-2 PALM (L)	-	0.00442	0.01560	2	5	24	14893	4.0038
Type-2 PALM (G)	-	0.00421	0.01487	3	5	36	14893	3.9134

[0.26, 0.31] correspondingly. The value of b_1 increases, and b_2 reduces compared to test 1, and the fewer number of rules are generated across different experiments of our work.

Table VII
SENSITIVITY ANALYSIS OF RULE GROWING THRESHOLDS

Parameters	NRMSE	NDEI	Execution time	#Rules
$b_2 = 0.055$	0.023	0.059	0.355	13
$b_2 = 0.054$	0.023	0.059	0.312	13
$b_2 = 0.053$	0.023	0.059	0.326	13
$b_2 = 0.052$	0.023	0.059	0.325	13
$b_1 = 0.020$	0.023	0.059	0.324	13
$l_2 = 0.022$	0.023	0.059	0.325	13
$b_1 = 0.024$	0.023	0.059	0.320	13
$b_1 = 0.026$	0.023	0.059	0.344	13
$b_1 = 0.037$	0.046	0.115	0.260	10
$b_1 = 0.035$	0.046	0.115	0.259	11
$b_1 = 0.033$	0.046	0.115	0.269	11
$b_1 = 0.031$	0.048	0.121	0.269	11
$b_2 = 0.050$	0.047	0.118	0.265	11
$b_2 = 0.048$	0.046	0.115	0.267	11
$b_2 = 0.046$	0.047	0.116	0.266	11
$b_2 = 0.044$	0.047	0.117	0.306	11

VII. CONCLUSIONS

A novel SANFS, namely PALM, is proposed in this paper for data stream regression. The PALM is developed with the

concept of HPBC which incurs very low network parameters. The reduction of network parameters bring down the execution times because only the output weight vector calls for the tuning scenario without compromise on predictive accuracy. PALM possesses a highly adaptive rule base where its fuzzy rules can be automatically added when necessary based on the SCC theory. It implements the rule merging scenario for complexity reduction and the concept of distance and angle is introduced to coalesce similar rules. The efficiency of the PALM has been tested in six real-world and artificial data stream regression problems where PALM outperforms recently published works in terms of network parameters and running time. It also delivers state-of-the art accuracies which happen to be comparable and often better than its counterparts. In the future, PALM will be incorporated under a deep network structure.

ACKNOWLEDGMENT

The authors would like to thank the Unmanned Aerial Vehicle laboratory of the UNSW at the Australian Defense Force Academy for supporting with the real-world datasets from the quadcopter and helicopter flight test, and Computational Intelligence Laboratory of Nanyang Technological University (NTU) Singapore for the computational support. This research

is financially supported by NTU start-up grant and MOE Tier-1 grant.

REFERENCES

- [1] C. C. Aggarwal, *Data streams: models and algorithms*. Springer Science & Business Media, 2007, vol. 31.
- [2] J. Gama, *Knowledge discovery from data streams*. CRC Press, 2010.
- [3] J. A. Silva, E. R. Faria, R. C. Barros, E. R. Hruschka, A. C. De Carvalho, and J. Gama, "Data stream clustering: A survey," *ACM Computing Surveys (CSUR)*, vol. 46, no. 1, p. 13, 2013.
- [4] R. J. C. Bose, W. M. Van Der Aalst, I. Zliobaite, and M. Pechenizkiy, "Dealing with concept drifts in process mining," *IEEE Transactions on Neural Networks and Learning Systems*, vol. 25, no. 1, pp. 154–171, 2014.
- [5] E. Lughofer and P. Angelov, "Handling drifts and shifts in on-line data streams with evolving fuzzy systems," *Applied Soft Computing*, vol. 11, no. 2, pp. 2057–2068, 2011.
- [6] C.-F. Juang and C.-T. Lin, "An online self-constructing neural fuzzy inference network and its applications," *IEEE Transactions on Fuzzy Systems*, vol. 6, no. 1, pp. 12–32, 1998.
- [7] P. P. Angelov and D. P. Filev, "An approach to online identification of Takagi-Sugeno fuzzy models," *IEEE Transactions on Systems, Man, and Cybernetics, Part B (Cybernetics)*, vol. 34, no. 1, pp. 484–498, 2004.
- [8] P. Angelov and D. Filev, "Simpl_eTS: A simplified method for learning evolving Takagi-Sugeno fuzzy models," in *The 14th IEEE International Conference on Fuzzy Systems, 2005. FUZZ'05*. IEEE, 2005, pp. 1068–1073.
- [9] M. Pratama, S. G. Anavatti, and E. Lughofer, "GENEFIS: toward an effective localist network," *IEEE Transactions on Fuzzy Systems*, vol. 22, no. 3, pp. 547–562, 2014.
- [10] M. Pratama, S. G. Anavatti, P. P. Angelov, and E. Lughofer, "PANFIS: A novel incremental learning machine," *IEEE Transactions on Neural Networks and Learning Systems*, vol. 25, no. 1, pp. 55–68, 2014.
- [11] M. Pratama, E. Lughofer, M. J. Er, S. Anavatti, and C.-P. Lim, "Data driven modelling based on recurrent interval-valued metacognitive scaffolding fuzzy neural network," *Neurocomputing*, vol. 262, pp. 4–27, 2017.
- [12] J. de Jesús Rubio, "Error convergence analysis of the sufin and csufin," *Applied Soft Computing*, 2018.
- [13] Y. Pan, Y. Liu, B. Xu, and H. Yu, "Hybrid feedback feedforward: An efficient design of adaptive neural network control," *Neural Networks*, vol. 76, pp. 122–134, 2016.
- [14] J. de Jesús Rubio, "Usnfnis: uniform stable neuro fuzzy inference system," *Neurocomputing*, vol. 262, pp. 57–66, 2017.
- [15] J. A. Meda-Campana, "Estimation of complex systems with parametric uncertainties using a jssf heuristically adjusted," *IEEE Latin America Transactions*, vol. 16, no. 2, pp. 350–357, 2018.
- [16] P. Angelov and R. Yager, "A new type of simplified fuzzy rule-based system," *International Journal of General Systems*, vol. 41, no. 2, pp. 163–185, 2012.
- [17] M. Pratama, P. P. Angelov, E. Lughofer, and M. J. Er, "Parsimonious random vector functional link network for data streams," *Information Sciences*, vol. 430, pp. 519–537, 2018.
- [18] E. Kim, M. Park, S. Ji, and M. Park, "A new approach to fuzzy modeling," *IEEE Transactions on Fuzzy Systems*, vol. 5, no. 3, pp. 328–337, 1997.
- [19] C. Kung and J. Su, "Affine Takagi-Sugeno fuzzy modelling algorithm by fuzzy c-regression models clustering with a novel cluster validity criterion," *IET Control Theory & Applications*, vol. 1, no. 5, pp. 1255–1265, 2007.
- [20] C. Li, J. Zhou, X. Xiang, Q. Li, and X. An, "T-S fuzzy model identification based on a novel fuzzy c-regression model clustering algorithm," *Engineering Applications of Artificial Intelligence*, vol. 22, no. 4-5, pp. 646–653, 2009.
- [21] M. F. Zarandi, R. Gamasae, and I. Turksen, "A type-2 fuzzy c-regression clustering algorithm for Takagi-Sugeno system identification and its application in the steel industry," *Information Sciences*, vol. 187, pp. 179–203, 2012.
- [22] W. Zou, C. Li, and N. Zhang, "A T-S Fuzzy Model Identification Approach based on a Modified Inter Type-2 FRCM Algorithm," *IEEE Transactions on Fuzzy Systems*, 2017.
- [23] R.-F. Xu and S.-J. Lee, "Dimensionality reduction by feature clustering for regression problems," *Information Sciences*, vol. 299, pp. 42–57, 2015.
- [24] J.-Y. Jiang, R.-J. Liou, and S.-J. Lee, "A fuzzy self-constructing feature clustering algorithm for text classification," *IEEE transactions on knowledge and data engineering*, vol. 23, no. 3, pp. 335–349, 2011.
- [25] wolfram, "Point-plane distance," 2018. [Online]. Available: <https://mathworld.wolfram.com/Point-PlaneDistance.html>
- [26] M. M. Ferdaus and M. Pratama, "PALM code," 2018. [Online]. Available: https://www.researchgate.net/publication/325253670_PALM_Matlab_Code
- [27] E. D. Lughofer, "FLEXFIS: A robust incremental learning approach for evolving Takagi-Sugeno fuzzy models," *IEEE Transactions on Fuzzy Systems*, vol. 16, no. 6, pp. 1393–1410, 2008.
- [28] N. K. Kasabov and Q. Song, "DENFIS: dynamic evolving neural-fuzzy inference system and its application for time-series prediction," *IEEE Transactions on Fuzzy Systems*, vol. 10, no. 2, pp. 144–154, 2002.
- [29] P. Angelov, "Evolving Takagi-Sugeno Fuzzy Systems from Streaming Data (eTS+)," *Evolving intelligent systems: methodology and applications*, vol. 12, p. 21, 2010.
- [30] A. Lemos, W. Caminhas, and F. Gomide, "Adaptive fault detection and diagnosis using an evolving fuzzy classifier," *Information Sciences*, vol. 220, pp. 64–85, 2013.
- [31] C.-F. Juang and Y.-W. Tsao, "A self-evolving interval type-2 fuzzy neural network with online structure and parameter learning," *IEEE Transactions on Fuzzy Systems*, vol. 16, no. 6, pp. 1411–1424, 2008.
- [32] C.-F. Juang, Y.-Y. Lin, and C.-C. Tu, "A recurrent self-evolving fuzzy neural network with local feedbacks and its application to dynamic system processing," *Fuzzy Sets and Systems*, vol. 161, no. 19, pp. 2552–2568, 2010.
- [33] C.-F. Juang and C.-Y. Chen, "Data-driven interval type-2 neural fuzzy system with high learning accuracy and improved model interpretability," *IEEE Transactions on Cybernetics*, vol. 43, no. 6, pp. 1781–1795, 2013.
- [34] N. N. Karnik, J. M. Mendel, and Q. Liang, "Type-2 fuzzy logic systems," *IEEE transactions on Fuzzy Systems*, vol. 7, no. 6, pp. 643–658, 1999.
- [35] C. J. Watkins and P. Dayan, "Q-learning," *Machine Learning*, vol. 8, no. 3-4, pp. 279–292, 1992.
- [36] R. H. Abiyev and O. Kaynak, "Type 2 fuzzy neural structure for identification and control of time-varying plants," *IEEE Transactions on Industrial Electronics*, vol. 57, no. 12, pp. 4147–4159, 2010.
- [37] S. Suresh, K. Dong, and H. Kim, "A sequential learning algorithm for self-adaptive resource allocation network classifier," *Neurocomputing*, vol. 73, no. 16-18, pp. 3012–3019, 2010.
- [38] M. Pratama, J. Lu, S. Anavatti, E. Lughofer, and C.-P. Lim, "An incremental meta-cognitive-based scaffolding fuzzy neural network," *Neurocomputing*, vol. 171, pp. 89–105, 2016.
- [39] R. J. Hathaway and J. C. Bezdek, "Switching regression models and fuzzy clustering," *IEEE Transactions on Fuzzy Systems*, vol. 1, no. 3, pp. 195–204, 1993.
- [40] R. Krishnapuram, H. Frigui, and O. Nasraoui, "Fuzzy and possibilistic shell clustering algorithms and their application to boundary detection and surface approximation. i," *IEEE Transactions on Fuzzy Systems*, vol. 3, no. 1, pp. 29–43, 1995.
- [41] S. Wu and M. J. Er, "Dynamic fuzzy neural networks—a novel approach to function approximation," *IEEE Transactions on Systems, Man, and Cybernetics, Part B (Cybernetics)*, vol. 30, no. 2, pp. 358–364, 2000.
- [42] P. Mitra, C. Murthy, and S. K. Pal, "Unsupervised feature selection using feature similarity," *IEEE Transactions on Pattern Analysis and Machine Intelligence*, vol. 24, no. 3, pp. 301–312, 2002.
- [43] L. Ljung, "System Identification, Theory for the User. Upper Saddle River, NJ 07458, USA, Prentice-Hall," ISBN 0-13-656695-2, Tech. Rep., 1999.
- [44] E. Lughofer, *Evolving fuzzy systems-methodologies, advanced concepts and applications*. Springer, 2011, vol. 53.
- [45] E. Lughofer, C. Cernuda, S. Kindermann, and M. Pratama, "Generalized smart evolving fuzzy systems," *Evolving Systems*, vol. 6, no. 4, pp. 269–292, 2015.
- [46] C.-H. Kim and M.-S. Kim, "Incremental hyperplane-based fuzzy clustering for system modeling," in *33rd Annual Conference of the IEEE Industrial Electronics Society, 2007. IECON 2007*. IEEE, 2007, pp. 614–619.
- [47] E. Lughofer, J.-L. Bouchot, and A. Shaker, "On-line elimination of local redundancies in evolving fuzzy systems," *Evolving Systems*, vol. 2, no. 3, pp. 165–187, 2011.
- [48] M.-S. Kim, C.-H. Kim, and J.-J. Lee, "Evolving compact and interpretable Takagi-Sugeno fuzzy models with a new encoding scheme," *IEEE Transactions on Systems, Man, and Cybernetics, Part B (Cybernetics)*, vol. 36, no. 5, pp. 1006–1023, 2006.

- [49] Y. Xu, K.-W. Wong, and C.-S. Leung, "Generalized RLS approach to the training of neural networks," *IEEE Transactions on Neural Networks*, vol. 17, no. 1, pp. 19–34, 2006.
- [50] P. Angelov, E. Lughofer, and X. Zhou, "Evolving fuzzy classifiers using different model architectures," *Fuzzy Sets and Systems*, vol. 159, no. 23, pp. 3160–3182, 2008.
- [51] D. J. MacKay, "Bayesian interpolation," *Neural Computation*, vol. 4, no. 3, pp. 415–447, 1992.
- [52] I. Goodfellow, Y. Bengio, A. Courville, and Y. Bengio, *Deep learning*. MIT press Cambridge, 2016, vol. 1.
- [53] M. M. Ferdous and M. Pratama, "RPALM code," 2018. [Online]. Available: https://www.researchgate.net/publication/325253670_RPALM_Matlab_Code
- [54] S. Wu, M. J. Er, and Y. Gao, "A fast approach for automatic generation of fuzzy rules by generalized dynamic fuzzy neural networks," *IEEE Transactions on Fuzzy Systems*, vol. 9, no. 4, pp. 578–594, 2001.
- [55] N. Wang, M. J. Er, and X. Meng, "A fast and accurate online self-organizing scheme for parsimonious fuzzy neural networks," *Neurocomputing*, vol. 72, no. 16-18, pp. 3818–3829, 2009.
- [56] M. C. Mackey and L. Glass, "Oscillation and chaos in physiological control systems," *Science*, vol. 197, no. 4300, pp. 287–289, 1977.
- [57] R. J. Oentaryo, M. J. Er, S. Linn, and X. Li, "Online probabilistic learning for fuzzy inference system," *Expert Systems with Applications*, vol. 41, no. 11, pp. 5082–5096, 2014.
- [58] J. Tan and C. Quek, "A BCM theory of meta-plasticity for online self-reorganizing fuzzy-associative learning," *IEEE Transactions on Neural Networks*, vol. 21, no. 6, pp. 985–1003, 2010.
- [59] FinanceYahoo.com, "S and p 500," 2018. [Online]. Available: <https://finance.yahoo.com/quote/%5EGSPC?p=%5EGSPC>
- [60] motion capture camera, "vicon camera," 2018. [Online]. Available: <https://www.vicon.com/>